Performance Test of the Air-Cooled Finned-Tube Supercritical CO2 Sink Heat Exchanger

Vojacekl, Ales; Dostal, Vaclav; Goettelt, Friedrich; Rohde, Martin; Melichar, Tomas

DOI
10.1115/1.4041686

Publication date
2019

Document Version
Final published version

Published in
Journal of Thermal Science and Engineering Applications

Ales Vojacek[1]
Research Centre Rez,
Hlavní 130,
Řež 250 68, Husinec, Czech Republic
e-mail: ales.vojacek@cvrez.cz

Vaclav Dostal
CTU in Prague,
Zikova 1903/4,
166 36 Prague 6,
Prague, Czech Republic
e-mail: Vaclav.Dostal@fs.cvut.cz

Friedrich Goettelt
XRG Simulation GmbH,
Harburger Schlossstraße 6-12,
Hamburg 21079, Germany
e-mail: gottelt@xrg-simulation.de

Martin Rohde
TU Delft,
Mekelweg 15,
JB Delft 2629, The Netherlands
e-mail: M.Rohde@tudelft.nl

Tomas Melichar
Research Centre Rez,
Hlavní 130,
Řež 250 68, Husinec, Czech Republic
e-mail: tomas.melichar@cvrez.cz

Performance Test of the Air-Cooled Finned-Tube Supercritical CO_2 Sink Heat Exchanger

This technical paper presents results of an air-cooled supercritical CO_2 (sCO_2) finned-tube sink heat exchanger (HX) performance test comprising wide range of variable parameters (26–166 °C, 7–10 MPa, 0.1–0.32 kg/s). The measurement covered both supercritical and subcritical pressures including transition of pseudocritical region in the last stages of the sink HX. The test was performed in a newly built sCO_2 experimental loop which was constructed within Sustainable Energy (SUSEN) project at Research Centre Rez (CVR). The experimental setup along with the boundary conditions are described in detail; hence, the gained data set can be used for benchmarking of system thermal hydraulic codes. Such benchmarking was performed on the open source Modelica-based code ClaRa. Both steady-state and transient thermal hydraulic analyses were performed using the simulation environment DYMOLA 2018 on a state of the art PC. The results of calculated averaged overall heat transfer coefficients (using Gnielinski correlation for sCO_2 and IPPE or VDI for the air) and experimentally determined values shows reasonably low error of + 25% and – 10%. Hence, using the correlations for the estimation of the heat transfer in the sink HX with a similar design and similar conditions gives a fair error and thus is recommended. [DOI: 10.1115/1.4041686]

Introduction

In the nuclear power plant design, the consideration of multiple component failure scenarios is a motivator for the development of failure safe backup systems. One approach for a failure safe backup system currently under development is called supercritical CO_2 heat removal (sCO_2-HeRo) [1]. It is designed for boiling water reactors and pressurized water reactors (PWRs) to prevent Fukushima-like accidents, where a combined station blackout, loss of ultimate heat sink, and loss of emergency cooling occurred. The sCO_2-HeRo is such an emergency cooling system. It transports the decay heat from the reactor core through a self-propellant, self-sustaining Brayton cycle, including compressor, heat exchanger (HX) (steam-sCO_2), turbine, and sink heat exchanger to the ambient air.

The main objective of this work was to provide evidence for the concept of the air-cooled finned-tube sink HX at laboratory conditions (technical readiness levels 3–4), develop and validate a new numerical Modelica-based model for the code ClaRa suitable for modeling steady/transient scenarios in sCO_2 environment, and finally deliver valuable operational experience from the unique sCO_2 facility at Research Centre Rez (CVR).

The measurement covered both the supercritical and subcritical pressures (7–10) MPa including transition of pseudocritical region (27–36) °C in the last stages of the sink HX. The nominal parameters of the sink HX were reached: 95 kW, 7.8 MPa, 166 °C/33 °C, 0.325 kg/s for the sCO_2 side cooled by 25 °C forced air flow with ambient pressure.

A number of investigators have carried out experimental tests and analyses of the heat transfer performance of finned-tube sCO_2 gas coolers. Majority of this work was focused only on steady-state analyses [1–4]. All of these authors use ε-NTU or LMTD (i.e., lumped method and distributed method) which has limitations, especially when it comes to modeling of rapidly varying thermophysical properties in the critical region. Therefore, e.g., LMTD has to be modified using an integral approach for LMTD [5] or finite methods need to be deployed, i.e., finite volume method utilized in this paper or finite element approach found in the work by Yin et al. [6] who performed stationary calculations and optimization.

Apart from an experimental research, there are numerous studies dedicated purely to simulation tools development for sCO_2 energy systems. In the dynamic simulation software, there can be found a few in-house system codes analyzing nuclear reactors and experimental loops behavior with sCO_2 [7,8] or system codes primary developed for light water reactors safety analyses like ATHLET, RELAP, and TRACE which has been upgraded for handling sCO_2 simulations [9–12]. However, the validation of these codes in sCO_2 environment has been lacking. Therefore, this study was conducted to present a new validated Modelica code as well as to submit a new set of sCO_2 data for future benchmark.

To the best of our knowledge there has been no previous investigations reported in the literature on the sCO_2 gas coolers performing experimental work together with both, the steady-state and transient analyses.

The results in this paper will benefit to researchers, designers, software engineers, thermal hydraulic specialists, and operators of sCO_2 energy systems through the shared measured data and described operational procedures in a unique sCO_2 facility.

Description of the sCO_2-Hero System. Figure 1 depicts the scheme of the sCO_2-HeRo retrofitted into the PWR. In case of a

[1]Corresponding author.

Contributed by the Heat Transfer Division of ASME for publication in the Journal of Thermal Science and Engineering Applications. Manuscript received April 4, 2018; final manuscript received October 2, 2018; published online February 11, 2019. Assoc. Editor: Cheng-Xian Lin.

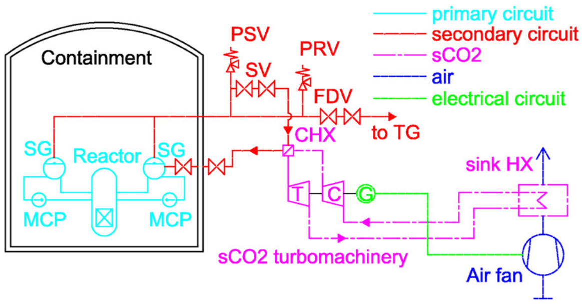

Fig. 1 SCO_2-HeRo system for a PWR

station black-out and the loss of ultimate heat sink accident, the reactor automatically shuts down, the turbine fast-driven valves close, and the safety valves open. However, the residual heat is produced. By nature, without the utilization of main circulation pump (MCP), natural circulation is established in the primary circuit, which transfers the decay heat to the steam generators (SG) and evaporates its water content. The steam flows into a heat exchanger (CHX), which must be very compact to fit into the limited space available in existing reactor building. The steam condenses and the liquid water, driven by gravity, flows back into the SG. Thus, the water content in the SG is preserved. Inside the compact HX the sCO_2 heats up. It flows through a turbine, which is located on the same shaft as the compressor and the generator. Downstream of the turbine, the sCO_2 gets cooled by the air in the sink HX and is delivered to the compressor and back to the compact heat exchanger. Over a large operating range, the turbine of the Brayton cycle shall produce more power than the compressor needs to operate. The excess power is transferred into electricity, which is used to power additional fans of the sink HX for better heat removal.

The sCO_2-HeRo system can be attached to both existing pressurized water reactors and boiling water reactors, since the thermodynamic parameters of steam are similar. Without having the sCO_2-HeRo system deployed, the water content in the SG would steadily decrease (by releasing the steam through pressure safety valve or pressure relief valve) causing overheating of the primary circuit which could eventually lead to fuel damage [13,14].

Within the European project "sCO_2-HeRo," six partners from three European countries are working on the assessment of this cycle. The goal is to numerically and experimentally show evidence for the concept on a small-scale demonstrator of the sCO_2-HeRo system which shall be incorporated in the PWR demonstrator (a reproduction of a two-loop pressurized water reactor Siemens/Kraftwerk Union design at a scale of 1:10) at the Simulator Centre of KGS and GfS in Essen, Germany. Before assembling the small sCO_2-HeRo system in the Simulator Centre, each major component was tested in different institutions. The performance of the compact HX (microchannel type) was verified in the sCO_2 test loop (SCARLETT) in University of Stuttgart, while the air-cooled sink HX, compressor, and turbine were measured in the CVR sCO_2 experimental facility.

Description of Sink HX for the Demonstrator

The design of the sink HX strongly influences the behavior of the whole sCO_2-HeRo system, as it is operated near the critical point region of CO_2 (7.8 MPa, 33 °C). Underestimated size of the HX can lead to a not self-propellant sCO_2-HeRo design. This is due to the high outlet temperature of the HX (inlet to the compressor) resulting in excessive compression work.

According to the optimized cycle calculations of the sCO_2-HeRo system, the sink HX model for the small scale sCO_2-HeRo has been specified [13].

Table 1 shows the main thermodynamic parameters for the selected two identical sinks HX's working in parallel. Each

Table 1 Thermodynamic parameters of sink HX

Variable	Value	Unit
Pressure of sCO_2 inlet to sink HX	78.3	bar
Temperature of sCO_2 outlet of sink HX	33.0	°C
Temperature of sCO_2 inlet to sink HX	166.0	°C
Mass flowrate of sCO_2	2×0.325	kg/s
Thermal power of sink HX	2×92.5	kW
Temperature of air inlet to sink HX	25.0	°C
Temperature of air outlet of sink HX	50.0	°C
Volumetric flowrate of air outlet	2×12500.0	m^3/h
Electric power of EC fans	2×0.33	kW

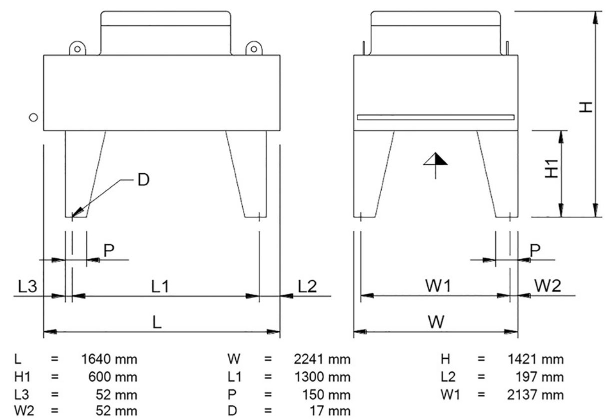

Fig. 2 Design of sink HX

designed as finned tube HX type cooled by forced air (fan with EC motor with speed control). One of them was selected for testing and implemented into the sCO_2 loop in CVR.

The conceptual drawing with overall dimensions is shown in Fig. 2.

The internals of sink HX includes stainless steel AISI 304 tubes in staggered arrangement with rectangular aluminum fins (metal sheet). The arrangement is such that the flow on the sCO_2 side is purely horizontal (except the inclined bends placed outside the air flow), while on the air side the flow is completely vertical. An illustrative scheme is shown in Fig. 3.

The overall heat transfer area for one sink HX is 361 m^2. The detail geometry of sink HX is included in Table 3.

Test Facility at Research Centre Rez

The heat transfer investigations in the sink HX test configuration took place at CVR, using sCO_2 experimental loop which was constructed within Sustainable Energy (SUSEN) project. This unique facility enables to study key aspects of the cycle (heat transfer, erosion, corrosion, etc.) with wide range of parameters:

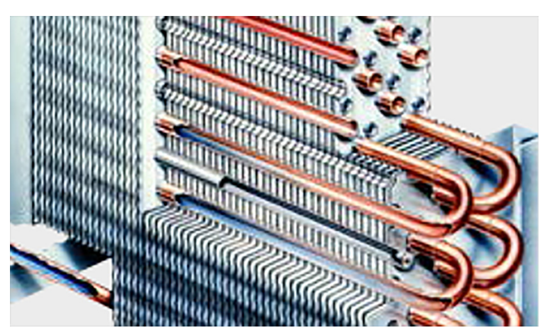

Fig. 3 Illustrative picture of the internals of sink HX including tubes with rectangular fins [15] (Reprinted with permission of Güntner GmbH & Co. KG © 2018)

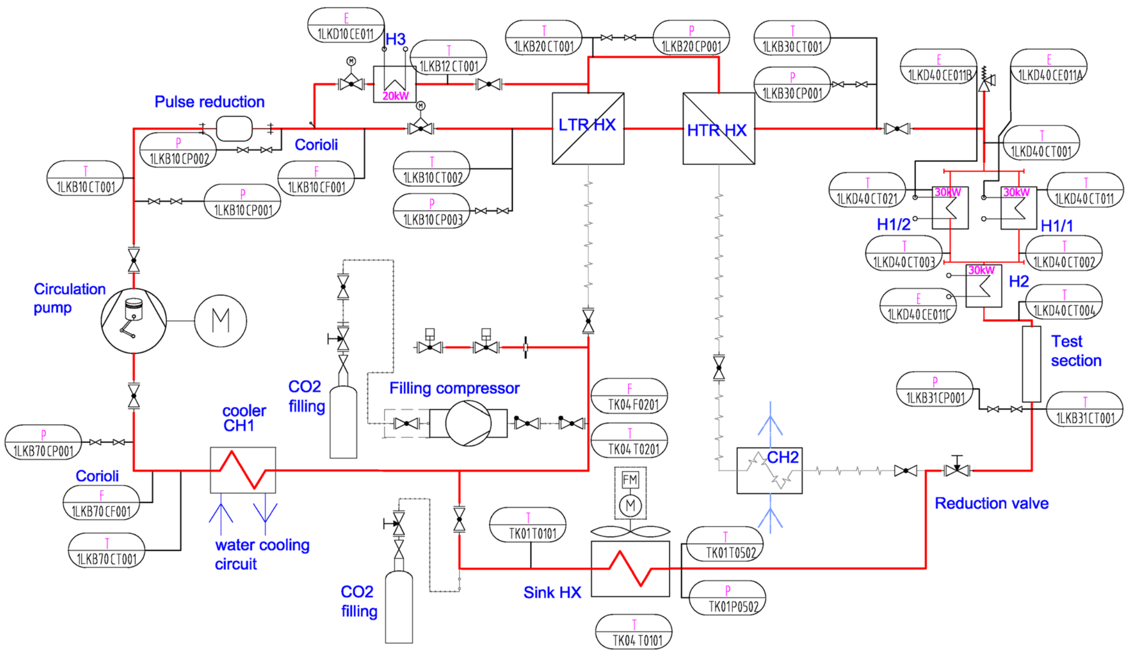

Fig. 4 Piping and instrument diagram of the sCO_2 loop with sink HX

Table 2 The main operating parameters of the sCO_2 primary loop

Name	Value	Unit
Maximum operation pressure	25	MPa
Maximum pressure in primary loop	30	MPa
Maximum operation temperature	550	°C
Maximum temperature in HTR	450	°C
Maximum temperature in LTR	300	°C
Nominal mass flow	0.35	kg/s

temperature up to 550 °C, pressure up to 30 MPa, and mass flow rate up to 0.35 kg/s.

Figure 4 shows the piping and instrument diagram (P&ID) of the loop. A part of the primary circuit used for the sink HX measurement is represented by thick line, and it consists of a low temperature regenerative heat exchanger (LTR) and high temperature regenerative heat exchanger (HTR), a main piston pump, and four electric heaters of the total maximum power of 110 kW. Heat exchangers HTR and LTR are designed as a counter-flow shell and tube-type from stainless steel (SS).

The electrical heater H3 with nominal power 20 kW is positioned at the bypass of the LTR in order to simulate the behavior of a recompression cycle.

For cooling purposes, two shell and tube type coolers CH_1 and CH_2 are connected to the loop. The cooler CH_1 from SS is cooled by water (temperature 20 °C, 1.4 kg/s flow rate of water), and the cooler CH_2 also from SS is used as the main cooling medium oil (Malotherm SH, Sasol, Sandton, South Africa), because of the high temperatures of the exhaust heat. Next part of the primary loop consists of two parallel electric heaters $H_{1/1}$ and $H_{1/2}$ from SS with 30 kW each, followed by one Inconel electrical heater H_2 with 30 kW. Behind the heaters, a test section TS (pressure tube which enables to insert samples) and reduction valve RV is positioned. It is used to represent a turbine expansion. The main operating parameters of the primary circuit are shown in Table 2.

For testing of the sink HX, the low pressure side (behind the reduction valve) of the LTR and the HTR as well as the oil cooler CH_2 were by-passed in order to achieve desired inlet temperatures (max. 170 °C) to the sink HX. The by-pass is marked in thick red line with squares. The omitted piping is marked in thin gray line. Pressure in the system is controlled either by the electric heaters, i.e., by the temperature in the circuit, or by the filling compressor/release valves (to the outside atmosphere) by which it is possible to control the amount of CO_2 in the loop, thus the pressure.

Table 3 Component geometry of the sCO_2 loop

Component	Geometry
Sink HX	Length = 1.4 m, width = 2.2 m, number of tubes = 8, number of rows in depths = 6, tube Ø 12 mm × 0.7 mm, number of passes = 5.5, length of a tube = 46.2 m long (1.4 × 6 × 5.5 = 46.2 m), thickness of fin = 0.5 mm, pitch between the fins = 2.4 mm, staggered arrangement, pitch s_1 = 50 mm, s_2 = 25 mm, and s_3 = 35 mm
HTR + LTR	Length of HTR = 20 m, length of LTR = 60 m, number of internal tubes = 7, internal tube Ø 10 × 1.5 mm, shell Ø 50 × 5 mm.
$H_{1/1} + H_{1/2}$	Length = 0.95 m, number of heating rods = 2 × 6, diameter of a heating rod = 8 mm, shell Ø 100 × 20 mm
H_2	Length = 0.95 m, number of heating rods = 2 × 6, diameter of a heating rod = 8 mm, shell Ø 73 × 6.5 mm
H_3	Length = 0.75 m, number of heating rods = 2 × 6, diameter of a heating rod = 8 mm, shell Ø 100 × 20 mm
CH_1	Length = 7.5 m, number of internal tubes = 7, internal tube Ø 10 × 1.5 mm, shell Ø 43 × 1.5 mm
CH_2	Length = 1.8 m, number of internal tubes = 7, internal tube Ø 10 × 1.5 mm, Shell Ø 43 × 1.5 mm
TS	Length = 1.5 m, shell Ø 73 × 6.5 mm
By-pass of sink HX	Length = 40 m, tube Ø 20 × 3 mm
Pipeline to sink HX	Length = 30 m, tube Ø 20 × 3 mm
Pipeline from sink HX	Length = 30 m, tube Ø 20 × 3 mm

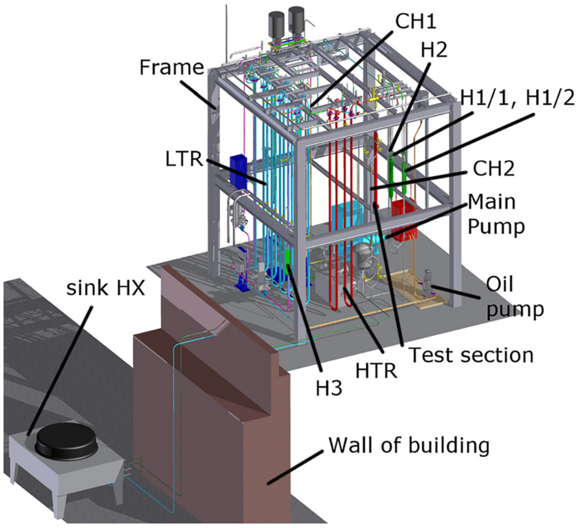

Fig. 5 Three-dimensional CAD model of the sCO_2 loop with sink HX modification

Figure 5 shows the sCO_2 loop and the installed sink HX configuration, which is outside of the experimental hall.

Component geometry of the sCO_2 loop is summarized in Table 3.

Measurements

This section contains the measurement procedure of the performed tests on sink HX within sCO_2 experimental facility in CVR.

Limits of the Test Facility at Research Centre Rez. Operational limits of the test facility (Table 4) must be taken into account and they should not be exceeded during the performance test.

For carrying out the experiments, the primary circuit was first evacuated and then filled by CO_2 (99.995%).

Figure 6 shows the sink HX outside of the experimental hall with in-coming and out-going pipelines together with all measurement devices.

Measurement Parameters and Procedure. The measurement campaigns covered both supercritical and subcritical regions including transition through the pseudocritical region in the last stages of the sink HX. The critical point of the CO_2 is 7.39 MPa and 31.1 °C. The controlled (independent) and resulted (dependent) parameters are summarized in Table 5.

Fig. 6 The sink HX with measurements

Measurement campaigns were carried out with different inlet conditions on both sides of the sink HX. The measurement time took about 15 min at each measurement point in order to reach stable conditions. The operational procedure was as follows:

(1) hold $p_{\_sCO2\_in} = 7.8$ MPa at nominal
(2) hold $\dot{m}_{\_sCO2}$ and $T_{\_sCO2\_in}$ at certain value (0.1, 0.2, or 0.32) kg/s and (50, 100, 166) °C, respectively
(3) vary $\dot{V}_{\_air\_out}$, i.e., frequency of the fan (50, 75, 100) % of nominal 50 Hz, while for each frequency a measurement was recorded

Table 4 Boundary conditions—test facility

Variable	Value	Unit	Description
p_{sCO2_max}	11.3	MPa	Maximum pressure of sCO_2 in the sink HX
T_{sCO2_max}	170	°C	Maximum temperature of the sink HX
$T_{\_air\_min}$	−30	°C	Minimum temperature of air in the sink HX
$T_{\_air\_max}$	55	°C	Maximum temperature of air at the outlet of the sink HX (fan limits)

Table 5 The main controlled and measured parameters for the performance tests

Variable	Value	Unit	Description
$p_{\_sCO2}$	7–10	MPa	Pressure—inlet of sCO_2 in the sink HX—controlled
$T_{\_sCO2\_in}$	50–166	°C	Temperature of sCO_2 inlet to the sink HX—controlled
$T_{\_sCO2\_out}$	25–37	°C	Temperature of sCO_2 outlet from the sink HX—measured
$\dot{m}_{\_sCO2}$	0.1–0.32	kg/s	Mass flow rate of the sink HX—controlled
$T_{\_air\_in}$	23–31	°C	Temperature of air inlet to the sink HX—[a]controlled
$T_{\_air\_out}$	31–65	°C	Temperature of air outlet from the sink HX—measured
$\dot{V}_{\_air\_out}$	6000–13,000	m^3/h	Volumetric flow rate of air outlet from the sink HX—controlled

[a]$T_{\_air\_in}$ depends on the actual ambient temperature.

Table 6 Installed measurement devices and errors

Variable	Range	Unit	Description	Device error	Transducer error	Input card error	Control system error	Total error
$\dot{m}_{\_sCO2}$	0–0.7	kg/s	Mass flow rate 1 LKB70CF001, Rheonik (RHM12)	0.15 % from 1.66 kg/s	Rawet—PX310S 0.1 % from range	Siemens SM 331 0.4 % from range	ABB freelance 0.1 % from range	±0.007 kg/s
New $T_{\_sCO2}$	0–200	°C	TC (type K) $T_{\_sCO2}$ with KKS starting with TK, Omega	0.275 % from range	Rawet—PX310S 0.1 % from range	Siemens SM 331 0.4 % from range	ABB freelance 0.1 % from range	±1.75 K
Existing $T_{\_sCO2}$	0–600	°C	TC (type K) $T_{\_sCO2}$ with KKS starting with LKB, Omega	0.25 % from range	Rawet—PX310S 0.1 % from range	Siemens SM 331 0.4 % from range	ABB freelance 0.1 % from range	±5.1 K
$p_{\_sCO2\_in}$	0–15	MPa	Pressure of the sCO_2 at the sink HX inlet, GE (UNIK 5000)	0.15 % from range	Rawet—PX310S 0.1 % from range	Siemens SM 331 0.4 % from range	ABB freelance 0.1 % from range	±0.11 MPa
$p_{\_sCO2}$	0–30	MPa	sCO_2 pressures at high pressure side of the loop starting with KKS LKB, GE (UNIK 5000)	0.15 % from range	Rawet—PX310S 0.1 % from range	Siemens SM 331 0.4 % from range	ABB freelance 0.1 % from range	±0.23 MPa
$P_{\_H1/1\text{-}2}$ $P_{\_H2,3}$	0–30	kW	Electric power of heaters, MT Brno	0.225 % from range	Rawet—PX310S 0.1 % from range	Siemens SM 331 0.4 % from range	ABB freelance 0.1 % from range	±0.4 kW
$T_{\_air}$	0–120	°C	Air temperature of sink HX inlet/outlet, JSP (Pt 100)	0.15 % from range	Rawet—PX310S 0.1 % from range	Siemens SM 331 0.4 % from range	ABB freelance 0.1 % from range	±0.82 K
$V_{\_air\_out}$	0–15,000	m^3/h	Wilson grid, AirFlow	5 % from range	Rawet—PX310S 0.1 % from range	Siemens SM 331 0.4 % from range	ABB freelance 0.1 % from range	±840 m^3/h

(4) increase/decrease $m_{\_sCO2}$ while keeping the $T_{\_sCO2\_in}$ and repeat step 3 and repeat this procedure for all variants of $\dot{m}_{\_sCO2}$ (0.1, 0.2 or 0.32) kg/s
(5) increase/decrease $T_{\_sCO2\_in}$ to new value and repeat steps 3 and 4 to record all variants of $T_{\_sCO2\_in}$ (50, 100, 166) °C

With this procedure the influence of $m_{\_sCO2}$, $T_{\_sCO2\_in}$, and $V_{\_air\_out}$ was studied. In order to see impact of $p_{\_sCO2\_in}$ following steps were taken:

(6) hold $T_{\_sCO2\_in}$ at certain value (100 °C)
(7) hold $m_{\_sCO2}$ and $p_{\_sCO2\_in}$ at certain value (0.1, 0.2, or 0.3) kg/s and (7, 7.4, 8.5, 9.4, 10) MPa, respectively, and vary $V_{\_air\_out}$
(8) increase/decrease $m_{\_sCO2}$ while keeping the $p_{\_sCO2\_in}$ and repeat step 3 repeat this procedure for all variants of $\dot{m}_{\_sCO2}$ (0.1, 0.2 or 0.32) kg/s
(9) increase/decrease $p_{\_sCO2\_in}$ to new value and repeat step 3 and 7 to record all variants of $p_{\_sCO2\_in}$ (7*, 7.4, 8.5, 9.4*, 10*) MPa.

*Not all $\dot{m}_{\_sCO2}$ (0.1, 0.2 or 0.32) kg/s were possible to implement due to the limited power of filling pump.

Measurement Devices and Experimental Errors. Figure 4 shows the piping and installation diagram (P&ID diagram) of the modified sCO_2 loop with the main components together with all installed measurement devices, such as a mass flow meter, volume flow meter, Pt-100 sensors, thermocouples, and pressure sensors. The nomenclature of the measurement devices respects the KKS identification system for power plants.

The uncertainties provided by the measurement devices, transducer, input card, and control system are summarized in Table 6. The errors correspond to calibration certificates and manufacturer's instructions.

The error propagations are described in Annex A.

The results for the design (nominal) conditions of the sink HX have shown 15% error propagation of the heat transfer on the sCO_2 side Q_{sCO2} and 8% for the air side $Q_{\_air.}$

Experimental Results and Discussion. This section contains experimental results for steady-state and transient operation.

Steady State Operation Results. Figure 7 shows the experimental results of $Q_{\_air} = \dot{m}_{\_air} \cdot c_{p\_air} \cdot (T_{\_air\text{-}out} - T_{\_air\_in})$ and $Q_{\_sCO2} = \dot{m}_{\_sCO2} \cdot (h_{\_sCO2-in} - h_{\_sCO2-out})$. For all of the 34 measurements, the heat transfer ratio $R = Q_{\_air}/Q_{\_sCO2}$ stayed within the limits (115%/85%). The base source of the errors propagation for the $Q_{\_sCO2}$ is the uncertainty of the thermocouple measurement of the outlet sCO_2 (far less than at the inlet). This is due to the fact that the pseudocritical region (around 34 °C) is crossed here and each small error of the temperature determination leads to high errors in evaluation of enthalpies (up to 60 kJ/kg), i.e.,

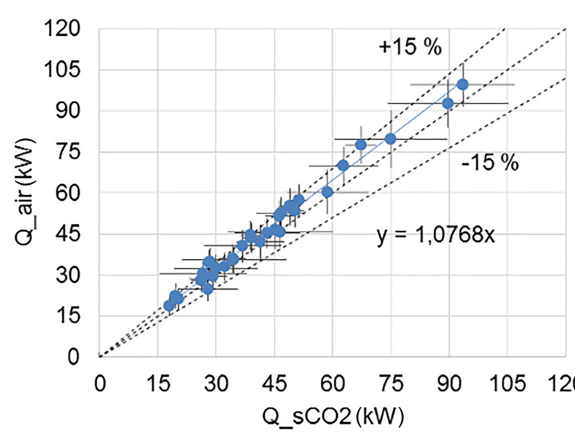

Fig. 7 Experimental results of *of Q*$_{air}$ *and Q*$_{sCO2}$ of the sink HX

heat power (15 kW). Figure 6 shows the sink HX standing outside of the experimental hall with pipelines and measurement devices.

The honey combs are utilized to stabilize the flow at the outlet of the air pipe and more importantly, in front of the Wilson grid which is used to measure volumetric flowrate throughout the pitot arrays. These consist of a row of vertical tubes, with alternate rows of holes facing up and down stream, measuring the total and substatic pressures from which dynamic pressures are calculated. As shown in Fig. 7, the air side heat flow rate $Q_{\_air}$ exceeds the CO_2 heat flow rate $Q_{\_sCO2}$. by max. 15%.

Comparison of Measurements With Correlations From the Literature. The potential of the sCO_2-HeRo system to deal with a range of different accident scenarios and beyond-design accidents will need to be proven with the help of thermal hydraulic codes. Therefore, heat transfer models were compared with the experimental data.

The heat transfer at the tube side where sCO_2 flows is geometrically characterized by the inner diameter and shape of the tubes and has been thoroughly studied. Numbers of correlations are discussed in the literature [16–18].

For calculating the local heat transfer coefficient on the inner side (sCO_2) of the heat exchanger, it is suitable to use well-known Gnielinski correlation for the forced convection [18]. Although, some investigators [19–21] modified this correlation, as indicated by Zilio et al. [22], these correlations often predict similar results for CO_2 gas coolers

$$\mathrm{Nu} = \frac{\frac{\zeta}{8}\cdot \mathrm{Re}\cdot \mathrm{Pr}}{1+12.7\cdot\sqrt{\frac{\zeta}{8}}\cdot\left(Pr^{\frac{2}{3}}-1\right)}\left(1+\left(\frac{d}{L}\right)^{\frac{2}{3}}\right)[-]\ \text{with}$$
$$\zeta = \left(1.8\cdot\log(\mathrm{Re})-1.5\right)^{-2}[-]$$
$$2300\le \mathrm{Re}\le 10^6 \quad 0.1\le \mathrm{Pr}\le 10^3 \quad \frac{d}{L}\le 1 \tag{1}$$

The air, which is pulled through the cooler by a fan mounted at the top of the unit, flows around the tube bundle with fins. This is geometrically much more complex. It includes definition of transverse and longitudinal tube spacing, tube outer diameter, number of tube rows, fin spacing, fin thickness, and fin type. Besides this complexity, the air local heat transfer coefficient is by one order of magnitude smaller than of the sCO_2 side. Thus, the air side determines the size of the whole HX.

Local heat transfer coefficient on the air side of the heat exchanger was calculated according to correlations for finned tubes. The Nusselt number was calculated such that the tubes are in staggered arrangement according to IPPE [23] and VDI [24]

$$\mathrm{Nu} = 0.192\cdot \mathrm{Re}_{d_{\mathrm{outer}}}^{0.65}\cdot\left(\frac{s_1}{s_2}\right)^{0.2}\cdot\left(\frac{h}{d_{\mathrm{outer}}}\right)^{-0.14}\cdot\left(\frac{u+\delta_{\mathrm{fin}}}{d_{\mathrm{outer}}}\right)^{0.18}$$
$$\cdot \mathrm{Pr}^{\frac{2}{3}}\cdot\left(\frac{\mathrm{Pr}}{\mathrm{Pr}_{\mathrm{fin}}}\right)^{0.25}[-]\quad \text{for}\quad 10^2\le \mathrm{Re}_{d_{\mathrm{outer}}}\le 2\times 10^4 \tag{2}$$

The following correlation cited in VDI is derived from confidential industrial data evaluation:

$$\mathrm{Nu} = 0.38\cdot \mathrm{Re}_{d_{\mathrm{outer}}}^{0.6}\cdot\left(\frac{A_{\mathrm{outer}}}{A_{\mathrm{tube}}}\right)^{-0.15}\cdot \mathrm{Pr}^{\frac{1}{3}}[-]\ \text{for}\ 10^3\le \mathrm{Re}_{d_{\mathrm{outer}}}\le 10^5 \tag{3}$$

The ideal coefficient of heat transfer at the air side α_{ideal} is then calculated from the Nusselt number using equivalent diameter d_{outer}. Since the design of the HX contains fins for increasing the heat transfer area, the real local heat transfer coefficient efficiency of the fin needs to be taken into account. The real local heat transfer coefficient is calculated according to the following equation:

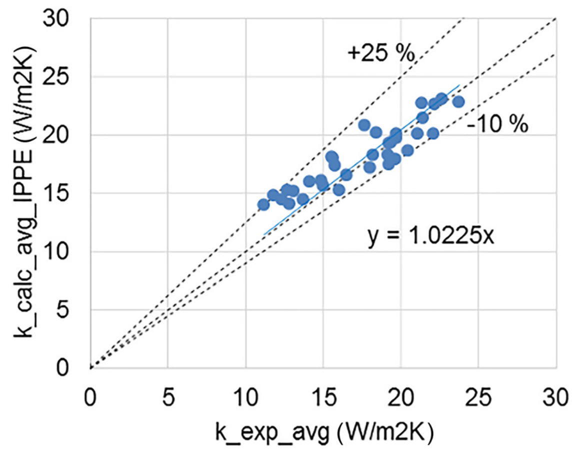

Fig. 8 Calculated the results of overall heat transfer coefficients $k_{\mathrm{calc\_avg\_IPPE}}$ (using IPPE correlation) and experimentally determined $k_{\mathrm{\_exp\_avg}}$ of the sink HX

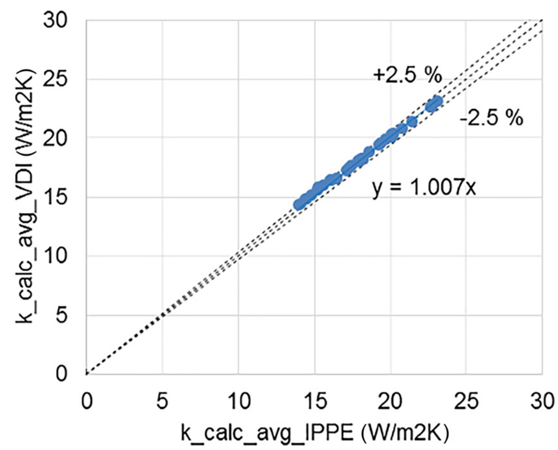

Fig. 9 A comparison of calculated results of overall heat transfer coefficients k_calc_avg according to IPPE and VDI

$$\alpha_{\mathrm{outer}} = \alpha_{\mathrm{ideal}}\cdot\frac{A_{\mathrm{fin}}}{A_{\mathrm{outer}}}\cdot\left(\eta_{\mathrm{fin}}+\frac{A_{\mathrm{outer\_tube\_fin}}}{A_{\mathrm{fin}}}\right)\quad (\mathrm{W/m^2K}) \tag{4}$$

For the calculation of efficiency of the rectangular fins η_{fin}, a formula stated in Ref. [24] was used. For the given geometry it resulted in $\eta_{\mathrm{fin}} = 0.95$.

The overall heat transfer coefficient k (W/m^2/K) was calculated according to the equation below:

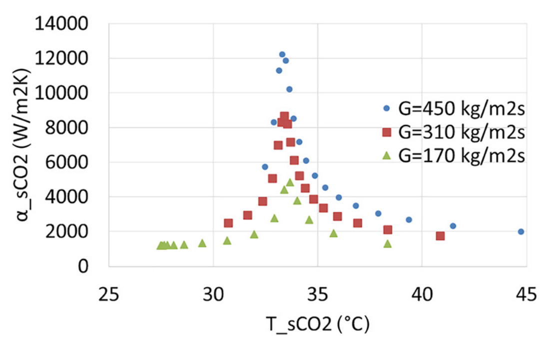

Fig. 10 Heat transfer coefficients versus sCO_2 temperature distribution along the gas coolers for different mass fluxes (p_{sCO2}=7.8 MPa, T_{pc} = 33.4 °C)

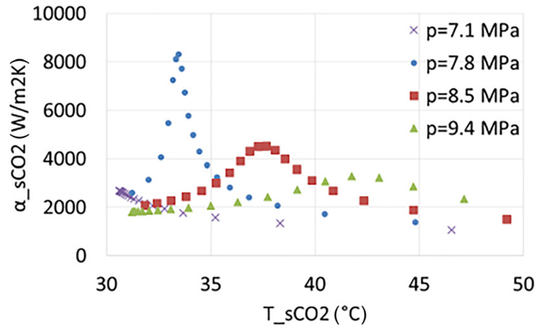

Fig. 11 Heat transfer coefficients versus sCO_2 temperature distribution along the gas coolers for different inlet pressures (T_{pc}(7.8 MPa) = 33.4 °C, T_{pc}(8.5 MPa) = 37.3 °C, T_{pc}(9.4 MPa) = 41.8 °C) at 0.2 kg/s

$$k = \frac{1}{\frac{1}{\alpha_{outer}} + \frac{A_{outer}}{A_{inner}} \cdot \left(\frac{1}{\alpha_{inner}} + \frac{\delta_{tube}}{\lambda_{tube}}\right)} \quad (\mathrm{W/m^2K}) \tag{5}$$

Equations (4) and (5) are taken from Refs. [24] and[25].

The graph in Fig. 8 shows a comparison of resulted averaged overall heat transfer coefficients $k_{\_calc\_avg}$ calculated (using Gnielinski [18] for sCO_2 and IPPE [23] for the air) and experimentally determined $k_{\_exp\_avg}$ for all the 34 measurement points. The overall $k_{\_exp\_avg}$ was calculated from the measured temperatures, pressures, mass flow rates on both the sCO_2 and air sides using the following formula $Q = k_{exp\_avg} \cdot A_{outer} \cdot \Delta T'(\mathrm{W})$ describing the heat transferred in each control volume of the sink HX. The positive errors suggest that the calculated values, using correlations, overestimate the experimental values for the negative errors and vice versa. It can be seen that the discrepancy is reasonable low—+25% and −10%.

From the graph Fig. 9, it can be concluded that both correlations according to IPPE and VDI are in perfect match.

The effect of the mass flux on the local heat transfer coefficient of sCO_2 is illustrated in Fig. 10. At the same pressure, the local heat transfer coefficient of sCO_2 increases with mass flux due to higher Reynolds number.

Figure 11 presents the local heat transfer coefficient of sCO_2 for different cooling pressures ranging from 7.1 MPa to 9.4 MPa at a given mass flux. For the supercritical pressures (higher than 7.4 MPa), the peak values in the local heat transfer coefficient are shown at the same pseudo-critical temperatures. Higher pressure has lower local heat transfer coefficient because the specific heat is lower. At the subcritical pressure (7.1 MPa), the local heat transfer coefficient increases toward colder temperatures and even exceeds the values of supercritical pressure due to the higher specific heat at this region. There has been considerable prior research done in the area of sCO_2 coolers with similar findings [20,21].

Table 7 Description of controlled parameters during transient scenario of sink HX

Time (s)	$\dot{m}$_sCO$_2$ (kg/s)	Time (s)	V_air_out (m^3/h)	Pressure control
Up to 1450	0.32	Up to 700	12,250	on
1470	0.3	720	9400	on
1600	0.3	1300	9400	on
1633	0.26	1320	6400	on
1704	0.26	1500	6400	on
1756	0.19	1520	12,500	off
1820	0.19	1900	12,500	off
1929	0.18	1900	0	off
1950	0.1	1950	0	off

Transient Operation. During the performance measurement of the sink HX a transient test was performed. The volumetric flow rate of the air was stepwise changed from the value 12,250 m^3/h through 9400 m^3/h (75% fan speed) to 6400 m^3/h (50% fan speed) while keeping the nominal sCO_2 mass flow rate at 0.32 kg/s. Before each change a steady-state was reached such that $p_{\_sCO2\_in} = 7.8$ MPa $T_{_sCO2_in} = 166\,°$C. Each drop of $V_{\_air\_out}$ resulted in a rise of pressure (2–4 bars) in the primary circuit due to a higher mean temperature in the system, particularly in the sink HX. This was compensated with the pressure control system feeding additional sCO_2 by a booster compressor. At time 1450 s (6400 m^3/h, 0.32 kg/s), frequency of the main circulation pump started to stepwise decrease the $\dot{m}_{\_sCO2}$. As consequence of the $\dot{m}_{\_sCO2}$ reduction, the inlet temperature to the sink HX $T_{\_sCO2\_in}$ abruptly increased, until it reached its maximum limit 170 °C at 1820s, even though the air fan was switched back to its nominal 100%. The automatic control system switched off all heaters which were at this time almost at their maximum, i.e., $H_{1/1}$—28 kW, $H_{1/2}$—30 kW, H_2—26 kW, and H_2—20 kW. Switching off the electric heaters resulted in sudden drops of the temperatures and pressures in the system. However, there was some reaction time of the control system, and the inlet temperature to the sink HX was slightly exceeded. The controlled parameters are summarized in Table 7.

Benchmark With Clara Numerical Code

The experimentally measured data of the sCO_2 loop from the transient scenario described in the Transient Operation section was used for code benchmark to test and validate thermal hydraulic Modelica-based code ClaRa [26,27].

ClaRa Source Code Overview. The pipe model includes equations derived from the general form of the conservation equations by the finite volume approach. The finite volume approach was used to derive a set of ordinary differential equations from partial differential equations, such that they can be implemented in a computer and numerically solved. In many situations (e.g., pipe model which is our case), it is reasonable to simplify models by restricting to one-dimensional mass flows which can be then spatially discretized and modeled by number of control volumes. For each control volume, we can write mass, momentum, and energy balance equations which are implemented in ClaRa.

Mass Balance

$$\frac{d\rho}{dt} = \frac{1}{V}(\dot{m}_{in} + \dot{m}_{out}) \tag{6}$$

Energy Balance

$$\frac{dh}{dt} = \frac{1}{\rho V}\left(V\frac{dp}{dt} - hV\frac{d\rho}{dt} + H_{flow_{in}} + H_{flow_{out}} + Q\right) \tag{7}$$

with $H_{flow\_in} = \dot{m}_{in} h_{in} \quad H_{flow\_out} = \dot{m}_{out} h_{out}$

Momentum Balance

$$0 = \Delta p_{geo} + \Delta p_{fric} + \Delta p_{adv} + (p_{in} - p) + (p_{out} - p) \tag{8}$$

ClaRa Source Code Extension. Numerical model of the finned tube HX type cooled by forced air has been implemented into the existing ClaRa pipe model. The numerical heat transfer was programed according to Eqs. (1)–(5). In order to determine the power of the fan, the pressure drop model of the HX on the air side was applied according to Ref. [23]

$$\Delta p = 0.5 \cdot \zeta \cdot n_{rows} \cdot \rho \cdot w^2 \tag{9}$$

For the staggered arrangement of the tubes the following correlations may be used:

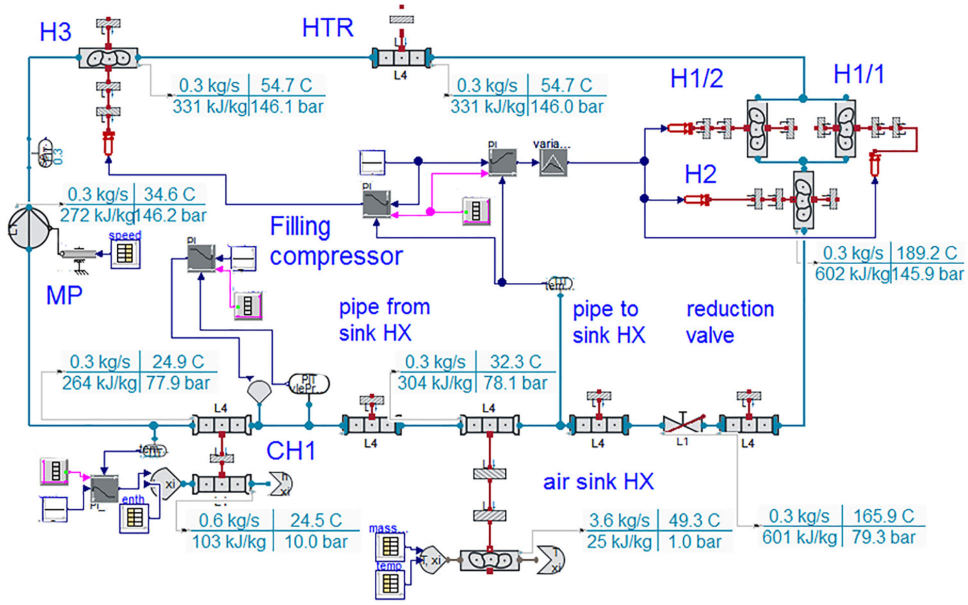

Fig. 12 Numerical model of the sink HX in Modelica with resulted nominal parameters

$$\zeta = 67 \cdot Re_{d_{\text{outer}}}^{-0.7} \cdot \left(\frac{A_{\text{outer}}}{A_{\text{tube}}}\right)^{0.5} \cdot \left(\frac{s_1}{d_{\text{outer}}}\right)^{-0.55} \cdot \left(\frac{s_2}{d_{\text{outer}}}\right)^{-0.5} \quad (10)$$

for $10^2 \le Re_{d_{\text{outer}}} \le 10^3$

$$\zeta = 3.2 \cdot \mathrm{Re}_{d_{\text{outer}}}^{-0.25} \cdot \left(\frac{A_{\text{outer}}}{A_{\text{tube}}}\right)^{0.5} \cdot \left(\frac{s_1}{d_{\text{outer}}}\right)^{-0.55} \cdot \left(\frac{s_2}{d_{\text{outer}}}\right)^{-0.5} \quad (11)$$

for $10^3 \le \mathrm{Re}_{d_{\text{outer}}} \le 10^5$

Description of the Test Facility Implementation With ClaRa. The dynamic sCO_2 loop model includes all major components of the CVR test facility according to the P&ID. The main circulation pump MP is speed-controlled with preset input parameters. Heaters with PID controllers provide desired temperatures at the sink HX. The outlet temperature of cooler CH_1 is handled with PID-operated water flow rate. The pressure in the system is controlled by feeding additional sCO_2 (by a booster compressor) or releasing sCO_2 through orifices, modeled in the computational model in a simple manner by the sCO_2 source, and the PID controller. The air flow rate through the sink HX is handled with defined input.

The obtained results of the computational model (Fig. 12) for the nominal parameters can be found in Fig. 13, where temperatures of the sCO_2 and air along the length of the sink HX tubes are displayed.

Results. The main resulted parameters from both, the measurement and transient simulation, are shown in Fig. 14. They show fair agreement, demonstrating reasonable accuracy of the simulation tool. There is an evident deviation at the peak inlet temperature of sCO_2 to the sink HX (by 13 K) leading to 3 bar pressure difference and 2 K discrepancy at the sink HX outlet. Apparently, this results from a smaller heat capacity of the numerical model than in reality. A faster temperature change (sCO_2) at the sink HX inlet justifies that. The model neglects all pipe supports, flanges, and bolts.

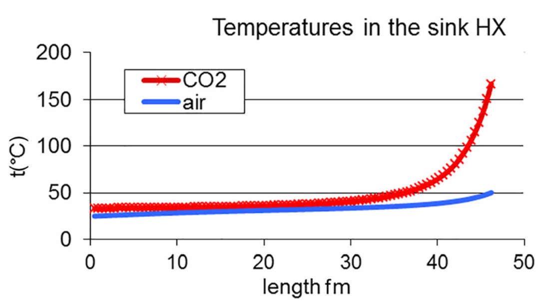

Fig. 13 Temperatures of the sink HX for nominal parameters

Conclusions

This paper reports the performance tests of the supercritical air-cooled finned-type sink HX (tube Ø 12 mm x 0.7 mm) and

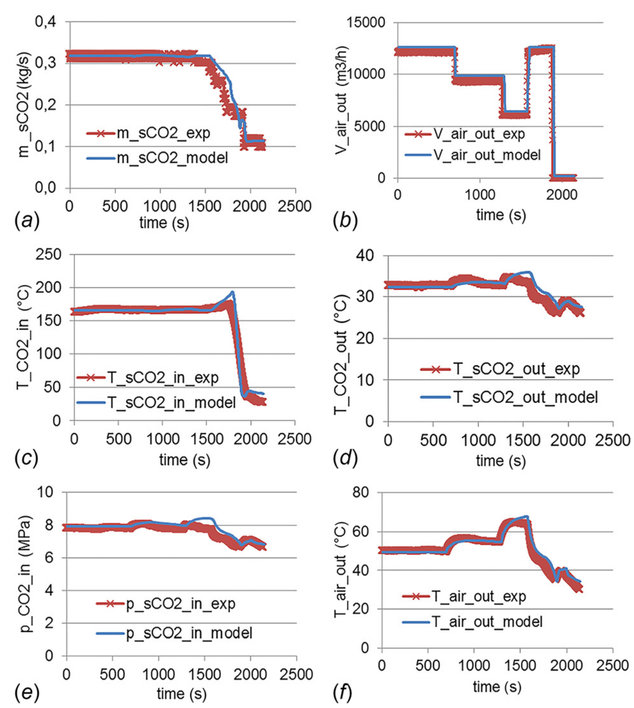

Fig. 14 Comparison of main resulted parameters from measurement and from simulation

presents a high quality numerical model. Altogether 34 measurement points were collected which were used for system code validation. Additionally, transients were logged, aiming to understand the energy and mass storage effects in the component.

The following conclusions can be drawn from the experimental results:

- The pressure, mass flux, and temperature of sCO_2 have significant effects on the local heat transfer coefficient, especially near pseudo-critical region. The local heat transfer coefficient is decreased when cooling pressure is increased (for $p_{sCO2} > 7.4$ MPa) otherwise increased when mass flux is increased. The local heat transfer coefficient along the sink HX changes rapidly with the temperature of the fluid. It reaches a peak near the pseudo-critical temperature due to the highest heat capacity.
- The experimentally determined heat balances from the measured parameters on both sides (sCO_2 and air) $Q_{\_air}$ and $Q_{\_sCO2}$ are in good agreement ($\pm 15\%$) with each other.
- The results of calculated averaged overall heat transfer coefficients $k_{\_calc\_avg}$ using correlations (Gnielinski [18] for sCO_2 and IPPE [23] or VDI [24] for the air) and experimentally determined values $k_{\_exp\_avg}$ show for the performed tests reasonably low error of $+25\%$ and -10%. Therefore, using the correlations for the estimation of the heat transfer in the sink HX with a similar design and similar conditions gives a fair error and thus is recommended. It is straightforward. Utilizing the measured data for look up tables for the HT of the sink HX is rather complicated to program.
- The analyzed correlations for heat transfer on the air side according to IPPE and VDI are in perfect match with each other.
- The sink HX heat exchanger configuration is able to remove planned 95 kW under design conditions, 7.8 MPa, 166 °C/33 °C, 0.325 kg/s (for the sCO_2 side) and 24 °C (design is 25 °C), 3.65 kg/s for the forced air flow with ambient pressure.
- Air-cooled finned-tube sink HX is suitable for the sCO_2-HeRo system.
- For a transient scenario—step-wise drop of $\dot{m}\_sCO_2$ followed by loss of electric heating power, a Modelica code with newly implemented sink HX model was used. Simulation matches the measurement results well with mean deviations ($\dot{m}_{\_sCO2}$ 5%, $\dot{V}_{\_air\_out}$ 5%, $T_{\_sCO2\_in}$ 2%, $T_{\_sCO2\_out}$ 3%, $p_{\_sCO2\_in}$ 3%, $T_{\_air\_out}$ 3%).

Acknowledgment

Authors thank Johannes Brunnemann and Timm Hoppe from XRG Simulation who provided insight and expertise of Modelica/ClaRa and wish to acknowledge the help of Martina Fruhbauerova with the final editing and proof read.

Funding Data

- European Union's Horizon 2020 research and training/research and innovation programme (662116/No 764690).
- Ministry of Education, Youth and Sport Czech Republic – project LQ1603 Research for SUSEN.

Nomenclature

A = area, m^2
c_p = specific heat capacity, J·kg^{-1}·K^{-1}
d = diameter, m
h = enthalpy, J·kg^{-1}
h' = height of fin, m
H_{flow} = enthalpy flow, W
K = overall heat transfer coefficient, W·m^{-2}·K^{-1}
L = length, m
$\dot{m}$ = mass flow rate, kg/s
n = number of fins of 1 tube
Nu = Nusselt number
p = pressure, Pa
P = electric power, W
Pr = Prandtl number
Q = heat power, W
Re = Reynolds number
s_1 = pitch of tubes perpendicular to the air flow direction, m
s_2 = pitch of tubes of HX above each other from the air flow sense, m
s_3 = pitch of tubes behind each other (diagonal) from the air flow sense, m
T = temperature, K
u = gap between fins of 1 tube, m
$\dot{V}$ = volumetric flow rate, m^3·s^{-1}
w = velocity, m/s
Δp = pressure drop, Pa
$\Delta T'$ = difference in temperatures of the mediums (air/sCO_2) within one segment of a heat exchanger, K

Greek Symbols

α = coefficient of heat transfer, W·m^{-2}·K^{-1}
β = auxiliary variable to calculate an efficiency of a fin
δ = thickness, m
ζ = pressure drop coefficient
η = dynamic viscosity, Pa·s
η_{fin} = efficiency of a fin
λ = thermal conductivity of a medium, W·m^{-1}·K^{-1}
ρ = density, kg·m^{-3}
σ_{cp} = error propagation of specific heat capacity, J·kg^{-1}·K^{-1}
σ_h = error propagation of enthalpy, J/kg
σ_m = error propagation of mass flow rate, kg·s^{-1}
σ_Q = error propagation of heat power transferred, W
σ_ρ = error propagation of density, kg·m^{-3}
$\sigma_{\dot{V}}$ = error propagation of volumetric flow rate, m^3·s^{-1}

Subscipts

air = air
adv = advection
calc_avg = calculated + averaged
cross = cross section
e = equivalent
exp_avg = experimentally determined + averaged
fin = fin of the heat exchanger
fric = frictional
grav = gravitational
h = hydraulic
$H_{1/1}$, $H_{1/2}$, H_2, and H_3 = heaters $H_{1/1}$, $H_{1/2}$, H_2, and H_3
Ideal = ideal (e.g., α_{ideal} is coefficient heat transfer for $\eta_{fin} = 1$)
in = inlet
inner = inner side (of tube/HX)
out = outlet
outer = outer side (of tube/HX)
outer_tube_fin = outer side among fins
sCO_2 = supercritical CO_2
tube = tube of the heat exchanger

Acronyms

CAD = computer-aided design
CH_1 = water cooler

CH_2 = oil cooler
CVR = Research Centre Rez
EC = electronically communicated
GfS = The Simulator Centre in Essen, Germany
$H_{1/1}$, $H_{1/2}$, H_2 and H_3 = electric heaters
HT = heat transfer
HTR = high temperature regenerative heat exchanger
HX = heat exchanger
IPPE = Institute of Physics and Power Engineering
KKS = identification system for power plants
LMTD = logarithmic mean temperature difference
LTR = low temperature regenerative heat exchanger
LWR = light water reactor
MP = main pump
MCP = main circulation pump
NTU = number of transfer unit
P&ID = piping and installation diagram
PID = proportional–integral–derivative
PWR = pressurized water reactor
sCO_2 = supercritical carbon dioxide
sCO_2-HeRo = supercritical carbon dioxide heat removal system
SG = steam generator
SS = stainless steel
SUSEN = Sustainable Energy project
TG = turbine generator
VDI = VDI - Heat Atlas

Appendix

When a function (e.g., enthalpy) is a set of nonlinear combination of the variables, an interval propagation could be performed in order to compute intervals which contain all consistent values for the variables. In a probabilistic approach, the function (e.g., enthalpy) must usually be linearized by approximation to a first-order Taylor series expansion.

Neglecting correlations or assuming independent variables (e.g., temperature and pressure) yields to a formula for a standard deviation of the function (e.g., enthalpy)

$$\sigma_h = \sqrt{\left(\frac{\partial h}{\partial T}\right)^2 \sigma_T^2 + \left(\frac{\partial h}{\partial p}\right)^2 \sigma_p^2 \ldots} \tag{A1}$$

The sCO_2 enthalpies at the inlet and outlet of the sink HX were calculated with RefProp [28] as a function of two independent parameters, the measured temperatures and pressures. Therefore, the sCO_2 inlet temperature $T_{\_sCO2\_in}$, the outlet temperature $T_{\_sCO2\_out}$, the inlet pressure $p_{\_sCO2\_in}$ and the outlet pressure $p_{\_sCO2\_out}$ were used. Due to the reason, that the enthalpy equation from RefProp is not available, the above-mentioned standard deviation equation was simplified to following:

$$\sigma_{h_{sCO2-in}} = \frac{\sqrt{\left(h_{\_sCO2\_in}\big|_{\frac{T_{\_sCO2\_in}}{p_{\_sCO2\_in\_max}}} - h_{\_sCO2\_in}\big|_{\frac{T_{\_sCO2\_in}}{p_{\_sCO2\_in\_min}}}\right)^2 + \left(h_{\_sCO2\_in}\big|_{\frac{T_{\_sCO2\_in\_max}}{p_{\_sCO2\_in}}} - h_{\_sCO2\_in}\big|_{\frac{T_{\_sCO2\_in\_min}}{p_{\_sCO2\_in}}}\right)^2}}{2} \tag{A2}$$

For the calculation of the sCO_2 enthalpy uncertainty at the inlet of the sink HX $\sigma_{h_{sCO2-in}}$ four enthalpies were used. The first one $h_{\_sCO2-in}|_{T_{\_sCO2\_in}/p_{\_sCO2\_in\_max}}$ was calculated with the measured sCO_2 inlet temperature $T_{\_sCO2\_in}$ and the maximum possible inlet pressure $p_{\_sCO2\_in\_max} = p_{\_sCO2\_in} + 0.11$ MPa, the second one $h_{\_sCO2-in}|_{T_{\_sCO2\_in}/p_{\_sCO2\_in\_min}}$ with the measured sCO_2 inlet temperature $T_{\_sCO2\_in}$ and the minimum possible inlet pressure $p_{\_sCO2\_in\_min} = p_{\_sCO2\_in} - 0.11$ MPa, the third one $h_{\_sCO2-in}|_{T_{\_sCO2\_in\_max}/p_{\_sCO2\_in}}$ with the measured sCO_2 inlet pressure $p_{\_sCO2\_in}$ and the maximum possible inlet temperature $T_{\_sCO2\_in\_max} = T_{\_sCO2\_in} + 1.75$ K and the fourth one $h_{\_sCO2-in}|_{T_{\_sCO2\_in\_min}/p_{\_sCO2\_in}}$ with the measured sCO_2 inlet pressure $p_{\_sCO2\_in}$ and the minimum possible inlet temperature $T_{\_sCO2\_min} = T_{\_sCO2\_in} - 1.75$ K. The propagated sCO_2 enthalpy uncertainty at the outlet of the sink HX $\sigma_{h_{sCO2-out}}$ was calculated in the similar manner as for $\sigma_{h_{sCO2-in}}$.

The heat power transferred from the sink HX at the sCO_2 was calculated as follows:

$$Q_{\_sCO2} = \dot{m}_{\_sCO2} * (h_{\_sCO2-in} - h_{\_sCO2-out}) \tag{A3}$$

It can be seen, that $Q_{\_sCO2}$ is a function of three independent parameters. According to the linearized Taylor-series and the propagation of uncertainty, for independent parameters, the error propagation $\sigma_{Q_{\_sCO2}}$ was calculated as follows:

$$\sigma_{Q_{sCO2}} = \sqrt{\left(\frac{\partial Q_{\_sCO2}}{\partial \dot{m}_{\_sCO2}} \sigma_{\dot{m}_{\_sCO2}}\right)^2 + \left(\frac{\partial Q_{\_sCO2}}{\partial h_{\_sCO2-in}} \sigma_{h_{sCO2-in}}\right)^2 + \left(\frac{\partial Q_{\_sCO2}}{\partial h_{sCO2-out}} \sigma_{h_{sCO2-Out}}\right)^2} \tag{A4}$$

The error propagation was repeated in similar manner for the air side

$$Q_{\_air} = \dot{m}_{\_air} c_{p\_air} (T_{\_air-out} - T_{\_air\_in}) \tag{A5}$$

$$\sigma_{Q_{\_air}} = \sqrt{\left(\frac{\partial Q_{air}}{\partial \dot{m}_{air}} \sigma_{\dot{m}_{air}}\right)^2 + \left(\frac{\partial Q_{air}}{\partial c_{p_{air}}} * \sigma_{c_{p_{air}}}\right)^2 + \left(\frac{\partial Q_{\_air}}{\partial T_{\_air\_out}} \sigma_{T_{\_air\_out}}\right)^2 + \left(\frac{\partial Q_{\_air}}{\partial T_{\_air\_in}} \sigma_{T_{\_air\_in}}\right)^2} \tag{A6}$$

References

[1] Brillert, D., 2015, "The Supercritical CO_2 Heat Removal System (sCO2-HeRo)," Faculty of Engineering, Chair of Turbomachinery, University of Duisburg-Essen, Duisburg, Germany, accessed Oct. 1, 2018, http://www.sco2-hero.eu/

[2] Ge, Y. T., Tassou, S. A., Santosa, I. D., and Tsamos, K., 2015, "Design Optimisation of CO2 Gas Cooler/Condenser in a Refrigeration System," Appl. Energy, **160**, pp. 973–981.

[3] Li, J., Jia, J., Huang, L. H., and Wang, S., 2017, "Experimental and Numerical Study of an Integrated Fin and Micro-Channel Gas Cooler for a CO_2 Automotive Air-Conditioning," Appl. Therm. Eng., **116**, pp. 636–647.

[4] Ho, D., Dang, T., Le, C. H., and Nguyen, T., 2017, "An Experimental Comparison Between a Microchannel Cooler and Conventional Coolers of a CO_2 Air Conditioning Cycle," International Conference on System Science and Engineering (ICSSE2017), Ho Chi Minh, Vietnam, July 21–23.

[5] Ngo, T. L., Kato, Y., Nikitin, K., and Ishizuka, T., 2007, "Heat Transfer and Pressure Drop Correlations of Microchannel Heat Exchangers With S-Shaped and Zigzag Fins for Carbon Dioxide Cycles," Exp. Therm. Fluid Sci., **32**(2), pp. 560–570.

[6] Yin, J. M., Bullard, W. B., and Hrnjak, P. S., 2001, "R-744 Gas Cooler Model Development and Validation," Int. J. Refrig., **24**(7), pp. 692–701.

[7] Carstens, N. A., Hejzlar, P., and Driscoll, M. J., 2005, "Description of Supercritical CO2 Systems Control Model," Center for Advanced Nuclear Energy Systems, MIT Nuclear Engineering Department, Cambridge, MA, Report No. MIT-GFR-027.

[8] Moisseytsev, A., and Sienicki, J. J., 2006, "Development of a Plant Dynamics Computer Code for Analysis of a Supercritical Carbon Dioxide Brayton Cycle Energy Converter Coupled to a Natural Circulation Lead-Cooled Fast Reactor," Argonne National Laboratory, Lemont IL, Report No. ANL-06/27.

[9] Driscoll, M. J., Hejzlar, P., and Apostolakis, G., 2008, "Optimized, Competitive Supercritical-CO_2 Cycle GFR for Gen IV Service," Center for Advanced Nuclear Energy Systems, MIT Nuclear Engineering Department, Cambridge, MA, Report No. MIT-GFR-045.

[10] Davis, C. B., Marshall, T. D., and Weaver, K. D., 2005, "Modelling the GFR with RELAP5-3D," RELAP5 International Users Seminar, Jackson Hole, WY, Sept. 7–9.

[11] Venker, J., 2015, "Development and Validation of Models for Simulation of Supercritical Carbon Dioxide Brayton Cycles and Application to Self-Propelling Heat Removal Systems in Boiling Water Reactors," Dr.-Ing thesis, Universitat Stuttgart, Stuttgart, Germany.

[12] Hexemer, M. J., and Rahner, K., 2011, "Supercritical CO_2 Brayton Cycle Integrated System Test (IST) TRACE Model and Control System Design," Supercritical CO2 Power Cycle Symposium, Boulder, CO, May 24–25.

[13] Vojacek, A., and Hakl, V., 2016, "Documentation System Integration Into European LWR Fleet, Deliverable No. 1.3; Horizon 2020—Fission Energy, The Supercritical CO_2 Heat Removal System," Confidential Report (Restricted to sCO2-HeRo Project Partners Only), accessed Oct. 23, 2018, http://www.sco2-hero.eu/results/deliverables/

[14] Venker, J., 2015, "Development and Validation of Models for Simulation of Supercritical Carbon Dioxide Brayton Cycle and Application to Self-Propelling Heat Removal Systems in Boiling Water Reactors," University of Stuttgart, Stuttgart, Germany, Report No. IKE2-156.

[15] GFHC - Güntner Fluid Cooler, 2018, "Guentner Condensers, Gas Coolers, and Fluid Coolers," Guentner, Schloßô Holte-Stukenbrock, Germany, accessed Oct. 1, 2018, https://www.guentner.eu/fileadmin/literature/europe/condensers_drycoolers/GFHC/Guentner_GCHC_GCVC_GGHC_GGVC_GFHC_GFVC_Info_EN.pdf

[16] Dostal, V., Driscoll, M. J., and Hejzlar, P., 2004, "A Supercritical Carbon Dioxide Cycle for Next Generation Nuclear Reactors," Center for Advanced Nuclear Energy Systems, MIT Nuclear Engineering Department, Cambridge, MA, Report No. MIT-ANP-TR-100.

[17] Hesselgreaves, J. E., 2001, *Compact Heat Exchangers – Selection, Design and Operation*, Pergamon, Amsterdam, London, New York, Oxford, Paris, Shannon, Tokyo.

[18] Gnielinski, V., 1976, "New Equations for Heat and Mass Transfer in Turbulent, Pipe and Channel Flow," Int. Chem. Eng., **16**(2), pp. 359–368.

[19] Pitla, S. S., Groll, E. A., and Ramadhyani, S., 2002, "New Correlation to Predict the Heat Transfer Coefficient During in-Tube Cooling of Turbulent Supercritical CO_2," Int. J. Refrig., **25**(7), pp. 887–895.

[20] Dang, C., and Hihara, E., 2004, "In-Tube Cooling Heat Transfer of Supercritical Carbon Dioxide—Part 1: Experimental Measurement," Int. J. Refrig., **27**(7), pp. 736–747.

[21] Oh, H. K., and Son, C. H., 2010, "New Correlation to Predict the Heat Transfer Coefficient in Tube Cooling of Supercritical CO2 in Horizontal Macro-Tube," Exp. Therm. Fluid Sci., **34**(8), pp. 1230–1241.

[22] Zilio, C., Cecchinato, L., Corradi, M., and Schiochet, G., 2007, "An Assessment of Heat Transfer Through Fins in a Fin-and-Tube Gas Cooler for Transcritical Carbon Dioxide Cycles," HVACR Res., **13**(3), pp. 457–469.

[23] Zukauskas, A. A., 1982, *Convective Transfer in Heat Exchangers*, Nauka, Moscow, Russia.

[24] 2010, *VDI- Heat Atlas*, 2nd ed., Springer-Verlag, Berlin.

[25] Vampola, J., 1984, "Heat Transfer and Pressure Drop in Finned-tube Bundles," State Research Institute for Machinery, Prague, Czech Republic.

[26] Modelica Association, 2000, "Modelica Language," Modelica Association, Linköping, Sweden, accessed Oct. 1, 2018, https://www.modelica.org/

[27] Lasse Nielsen TLK-Thermo GmbH, 2013, "dynstart | ClaRa – Simulation of Clausius-Rankine cycles | TLK-Thermo GmbH, Braunschweig | XRG Simulation GmbH, Hamburg | Institut für Thermofluiddynamik (TUHH), Hamburg | Institut für Energietechnik (TUHH), Hamburg." accessed Oct. 1, 2018, https://www.claralib.com/

[28] REFPROP National Institute of Standards and Technology (NIST), 2013, "Thermophysical Properties Division," REFPROP National Institute of Standards and Technology (NIST), Boulder, CO.